

Fugitive Emissions from a Dry Coal Fly Ash Storage Pile

Stephen F. Mueller, Qi Mao, Ralph J. Valente and Jonathan W. Mallard
Tennessee Valley Authority, P.O. Box 1010, Muscle Shoals, AL 35662
sfmueller@tva.gov

Stephanie L. Shaw
Electric Power Research Institute, 3420 Hillview Avenue, Palo Alto, CA 94304
sshaw@epri.com

ABSTRACT

Standardized estimates of fugitive emissions resulting from bulk materials handling are subject to many potential uncertainties based on the material of interest, the specifics of operational handling, and local geography and meteorology. In 2011 EPRI undertook the first of 3 phases of a field monitoring study at a power plant that investigated fugitive emissions of $PM_{2.5}$ and $PM_{10-2.5}$ (“ PM_c ” for short) from a large dry storage coal fly ash pile. The results incorporated ambient measurements from May to October of 2011, statistical analyses of meteorological data, use of dispersion modeling to calculate emission factors, and a comparison to AP-42 approaches. Specifically, hourly $PM_{2.5}$ and PM_{10} data from beta attenuation monitors (BAMs) was combined with high frequency measurements of light scattering (b_{scat}) to make measurements of background concentrations as well as two sites downwind of a dry fly ash pile at a large coal-fired power plant. Activities monitored on the dry stack included hauling, dumping, and grading. In addition, an unpaved road exists along the base of the dry stack on top of a berm to stabilize the stack. This road is a source of vehicle-generated fugitive dust, and methods were developed to separate out the contribution from the fly ash emissions signal. The results suggest $PM_{2.5}$ and PM_c emission factors for both fly ash and road dust that are considerably lower than those based on AP-42 methods. Planned future work includes similar studies of coal and limestone/gypsum materials.

INTRODUCTION

The United States Environmental Protection Agency (EPA) defines fugitive emissions in Title V (parts 70 and 71) of the Clean Air Act as emissions that cannot “reasonably pass through a stack, chimney, vent, or other functionally-equivalent opening” (see Code of Federal Regulations--CFR). This definition includes gases, liquid droplets and solid particulate matter. Emissions streams that pass through a vent, stack or chimney are confined making them relatively easy to sample. By contrast, fugitive emissions are not confined and that makes quantifying them a challenge.

Despite the difficulties measuring them, fugitive emissions can often comprise a large portion of the total emissions associated with a source that is required to obtain an air permit. Fugitive particulate emissions (hereafter, “fugitive emissions”) can also be difficult to control. They must be considered when determining whether a source adversely impacts ambient air quality standards. In addition, fugitive emissions must be addressed for new source review and prevention of significant deterioration impacts for electric generating units larger than 250 million BTU per hour heat input (CFR title 40, part 51, §166). In some cases fugitive emissions modeling may be required. Accurate emissions estimates can keep annual emission estimates below the threshold for modeling. Therefore, fugitive emissions are an important air pollution issue. Quantifying fugitive emissions is especially important to source operators that handle granular materials (e.g., coal, fly ash, limestone) or that operate vehicles on unpaved surfaces.

Quantifying fugitive emissions for air permitting purposes generally relies on published emission factors. These factors relate the amount of particulate material emitted into the air from a specific

process to some more easily quantifiable aspect of the process. For example, a formula exists (EPA, 1995 and subsequent updates) that estimates the amount of fugitive emissions associated with the dumping of a load of material from a dump truck or similar material conveyor. The value determined in this manner--expressed as mass of particulate matter emitted per mass of material deposited--is an emissions factor (EF).

This paper describes a study designed to quantify fugitive EFs for particles smaller than 10 and 2.5 micrometers (PM₁₀ and PM_{2.5}, respectively) associated with dry fly ash disposal at a coal-fired power plant. The intent of this work was to develop EFs specific to fly ash storage activities and compare them with EFs derived using standard formulations in the EPA AP-42 emissions handbook (EPA, 1995 and subsequent updates).

PREVIOUS WORK

One of the earliest (if not the first) comprehensive compilations of particulate fugitive EFs was made by Cowherd et al. (1974) for the EPA. The authors cite several references that describe prior efforts to quantify fugitive emissions from roads, tillage and material storage piles. All approaches to quantifying fugitive emissions used measurements of airborne particles, or particle deposition plus dispersion/deposition estimates, to link measured downwind concentrations or deposition back to emission rates. Some focused on suspended particles across a large size range (3-100 μm in diameter) whereas others collected data specifically on smaller particles (in the 1-10 μm range). The largest particles--especially those $>30 \mu\text{m}$ --tended to deposit quickly and could be captured by simple "dustfall" collectors. Smaller particles were collected on filters from sampling air streams.

Most research described by Cowherd et al. (1974) focused on fugitive emissions from paved and unpaved (dirt and gravel) roads. They reported unpaved road fugitive emissions of between 0.5 and 13.9 pounds per vehicle mile travelled (lb/VMT) for total particle concentrations, between 0.4 and 5.2 lb/VMT for particles smaller than 10 μm , and between 0.11 and 0.43 lb/VMT for particles smaller than 2 μm . Cowherd et al. (1974) conducted their own fugitive dust studies. Data were available to evaluate fugitive emissions as a function of precipitation, wind speed, aggregate size and activity levels. Cowherd et al. concluded that wind speed was not a major factor (i.e., wind erosion of dust from storage piles was not important). Also, aggregate size was not found to be a predictor of fugitive emissions. Only wetness ("wet" days were defined as those receiving rainfall on the day before or the day of sampled operations) and activity level at the site were significant predictors of fugitive emissions. Estimated EFs across all particle sizes averaged 0.42 lb/ton of material handled ("ton" denotes the weight unit =2000 pounds).

Separate measurements were made by Cowherd et al. (1974) near a contrived aggregate off-loading operation using a pile of crushed limestone and a rented front loader. Analysis produced an estimated EF of 0.11 lb/ton of limestone processed and the airborne dust had a mass mean diameter of 1.4 μm .

The updated version of the EPA AP-42 handbook contains numerous references to studies of unpaved and paved road fugitive emissions. The only reference from a peer-reviewed (and thus, readily accessible) source is Dyck and Stuckel (1976) who describe an experiment in which a 4.5 ton flatbed truck carrying different weight loads drove along a dry unpaved dirt road while high volume particulate samplers were operated at varying locations upwind (for background samples) and downwind (4 between 15 and 76 m). Truck speeds--held steady during each experiment--were varied between 4.5 to 11.2 m sec^{-1} . Truck weight was varied between 3900, 5700 and 7500 kg and three road types were tested. Multivariate regressions were done to determine relationships between EF, truck weight, truck speed, road silt content, road surface moisture content and wind speed. Dyck and Stuckel (1976) computed the fugitive emission rate using a dispersion equation for an infinite line source, measured one hour particle concentrations, the number of truck passes per hour and meteorological data collected nearby. Variations in road moisture content had no effect on computed EFs but this is probably because

the tests were only conducted during dry conditions. The results suggested a linear relationship between the fugitive EF for dust and the predictors of vehicle weight, speed, silt content and road type:

$$\text{Equation (1)} \quad E_{D\&S} = 5.286 - 3.599 R + 0.00271 VWS$$

where R is road type (=0 or 1), V is vehicle speed (miles per hour), W is vehicle weight (tons) and S is road surface silt content (percent). At a speed of about 12 m sec⁻¹, with road silt of 5-20 percent and for the vehicle weights used in the Dyck and Stuckel experiments, equation (1) yields EFs of between 5 and 30 lb/VMT, similar to those reported by Cowherd et al. (1974). Dyck and Stuckel results for fugitive emissions on unpaved industrial roads were incorporated into the AP-42 handbook.

The AP-42 handbook is the widely accepted authoritative source in the United States for estimating EFs of all types of sources and pollutants, evolving as new data become available. The current version lists EFs for various activities, including vehicles travelling on unpaved roads (two methods) and off-loading (dumping or dropping) of aggregate material. These are important in the current context because we examine EFs specific to dry fly ash disposal (an operation that includes vehicles driving on unpaved surfaces and material dropping). Fugitive emissions associated with wind erosion emissions are not considered by this study because measured wind speed never met the erosion threshold criteria in AP-42.

Material dropping operations were quantified by an EPA-sponsored study in the 1980s. The AP-42 handbook (Section 13.2) assigns the EF formulation (factor E_{drop}) an "A" rating for the highest level of certainty. Factor E_{drop} is represented by

$$\text{Equation (2)} \quad E_{drop} = 0.0016 k_{drop} \frac{(U/2.2)^{1.3}}{(M/2)^{1.4}}$$

where k_{drop} is a dimensionless particle size fraction multiplier, U is wind speed (m sec⁻¹) and M is the material moisture content (in percent). Units of E_{drop} are kilograms of airborne particles emitted per megagram of material dropped. AP-42 defines k_{drop} as 0.74 for particles <30 μm, 0.35 for particles <10 μm and 0.053 for particles <2.5 μm. AP-42 cautions that equation (2) is most applicable when dropping conditions fall within the range of conditions that occurred during the study on which equation (2) is based, as follows: material silt content S of between 0.44 and 19 percent, $0.25 \leq M \leq 4.8$ percent, and $0.6 \leq U \leq 6.7$ m sec⁻¹.

EFs for vehicles on unpaved roads are also described in AP-42 Section 13.2. Two formulations are given, one for traffic on public roads and one for vehicles driving at industrial sites. These formulations are based on work described in Cowherd et al. (1974), Dyck and Stukel (1986) and four other obscure references. Traffic on public roads is assumed to be primarily from automobiles and small trucks whose speeds are assumed to vary over a larger range than that for heavy trucks at industrial sites. Thus, the public road formulation allows for vehicle speed but neglects vehicle weight. The opposite is true for the industrial site formulation. Both unpaved road formulations are assigned a quality rating of "B" (one level below the rating for the dropping formulation) but the designation degrades if conditions fall outside those used to derive the formulations.

For industrial unpaved roads or surfaces the AP-42 EF E_{ir} is given as

$$\text{Equation (3)} \quad E_{ir} = 0.282 k_{ir} \left(\frac{S}{12}\right)^a \left(\frac{W}{3}\right)^{0.45}$$

with k_{ir} being a dimensionless particle size fraction parameter [different from k_{drop} in equation (2)], W is vehicle weight (in tons) and exponent $a = 0.9$ for particles smaller than 10 μm. Values for k_{ir} are 1.5 for the PM₁₀ mass fraction and 0.15 for the PM_{2.5} fraction. Units of E_{ir} are kilograms of airborne particles emitted per vehicle kilometer traveled. Likewise, The AP-42 formulation for E_{pr} (public unpaved roads) is

$$\text{Equation (4)} \quad E_{pr} = 0.282 \left[k_{pr} \frac{(S/12)(V/30)^d}{(M/0.5)^c} - C \right]$$

with $k_{pr} = 1.8$ for the PM_{10} mass fraction and 0.18 for the $PM_{2.5}$ fraction. Exponents c and d are given as 0.2 and 0.5, respectively, for all particles <10 μm . Vehicle speed (V) is in units of miles per hour but the conversion factor has been included in equation (4) to produce E_{pr} in metric units. Parameter C is included to remove the contributions of vehicle fleet exhaust and brake and tire wear that were combined with road dust in the field experiments performed to derive equation (4). AP-42 gives C as 0.00047 and 0.00036 lb/VMT for PM_{10} and $PM_{2.5}$, respectively.

The primary applicability of equation (3) is for $2 \leq S \leq 25$ percent, $2 \leq W \leq 290$ tons, $V < 70$ km hr^{-1} and $M \leq 13$ percent. Likewise, the applicability of equation (4) is primarily for $2 \leq S \leq 35$ percent, $1.5 \leq W \leq 3$ tons, $16 \leq V \leq 88$ km hr^{-1} and $M \leq 13$ percent. Thus, equation (3) is applicable over a much greater vehicle weight range than equation (4) whereas equation (4) is applicable over a greater vehicle speed range than equation (3). These limitations must be remembered when interpreting later comparisons between EFs. Note that just because W does not appear in equation (4) and V does not appear in equation (3) does not mean that fugitive emissions under those conditions do not respond to W and V . Data scatter tends to be large with these kinds of relationships and it is likely that parameters exhibiting relatively small variations do not become significant predictors when multivariate statistical analyses are performed.

EXPERIMENTAL METHOD

Approach

The method used to quantify fly ash disposal EFs was--like previous studies--inferential and based on ash handling information, meteorological data and a transport/diffusion model to link source activity with measured downwind concentrations. An illustration of the monitoring approach is provided in Figure 1. Air sampling downwind of the fly ash storage area collected data that included impacts from both fly ash and unpaved road dust. Light scattering (so-called " b_{scat} ") data detected the presence of particle plumes and airborne particle samplers provided information on particle mass concentrations for two particle size ranges. Digital photographs and statistical methods were used to remove the influence of road and construction dust allowing quantification of the fly ash influence. Records and other observations on ash handling enabled a coupling of simulated (using the atmospheric dispersion model) dust emission estimates with on-site ash handling activity.

The field measurement campaign was conducted at the 1200 MW Colbert coal-fired electric generating plant operated by the Tennessee Valley Authority in northwest Alabama. Colbert does not operate SO_2 removal technology and currently burns about 8900 tons of low-sulfur coal daily. Fly ash and water are moved as slurry to hoppers that hold it for transport to the disposal area (the so-called "dry stack"). The wet ash is transferred to ~30-ton haul trucks that transport it about a mile to the disposal site. At the dry stack the ash is dumped onto the top of the stack and spread into a pile of uniform height. The stack top is currently about 20 m above the surrounding ground level and the active disposal area covers roughly 3.2 hectares. The terraced sides of the dry stack are covered with short grass. Occasionally, as the ash level rises the exposed outer edge of the ash is covered in clay, an activity that is very infrequent and did not occur during periods analyzed for fugitive emission rates.

Activity logs provide data on the daily amount of fly ash moved to the dry stack, the number of truck loads hauled, and whether other materials were handled at the site. The fly ash disposal foreman reported that each load of ash dumped is leveled by a grader to a depth of 18-24 inches (0.46-0.61 m). Given the typical volume of ash per truck load, this is equivalent to a circular pile about 3.5 m in radius. Each load requires an average of 8 min for pile leveling work. The average speed of the grader is 5 miles per hour (2.2 m sec^{-1}). This speed constrains the distance traveled by the grader while processing a load to about 1000 m. The processing time allows a maximum of about 7-8 ash loads deposited per hour. However, in some cases up to 12 loads were deposited per hour. We assumed that the grading activity was slightly more efficient during the peak periods (i.e., less than 8 min was needed to level a

pile) but that some grading work continued into the next hour. The foreman also reports that piles are typically dumped in contiguous areas which allows for the most efficient means of leveling multiple piles and constrains the ash dumping/processing activities to only a small portion of the dry stack top on any given day. This information was used to model fugitive fly ash dispersion from the storage area and to compute EFs using AP-42 formulations.

Measurements

Detailed meteorological data were collected to characterize site weather (especially rainfall), airflow variations by direction, atmospheric turbulence and turbidity. The latter data were critical in detecting particle plumes from nearby fugitive dust sources. Except for the nephelometer (for light scattering measurements) the meteorological instruments were deployed on or near a 10-m tower (Figure 2) in a grassy field located north of the fly ash dry stack. The field had a slight (~4 percent) positive elevation gradient from southeast to northwest. This put the base of the tower (located about 60 m northwest of monitoring Site 2) at an elevation about 2-3 m above Site 2. Temperature, relative humidity and 3-dimensional airflow (using sonic anemometers) were measured at 2.3 and 9.6 m above the ground. A net radiometer was mounted at the lower tower level and a tipping bucket rain gauge was located about 6 m from the tower.

Particle concentration data were needed to calculate the contributions of fugitive sources to total concentrations of PM_{10} (C_{PM10}) or $PM_{2.5}$ ($C_{PM2.5}$). These measurements were made hourly using Met One beta attenuation monitors (BAMs), a Federal Equivalence Method instrument, located at three sites. Measurements at Site 1 (not shown in Figure 2) represented background conditions and Sites 2 and 3 were downwind of the fly ash disposal area when winds had a southerly component. Similar instrumentation has been deployed elsewhere to measure fugitive dust impacts (Watson et al., 2011). Particle mass was also collected using BGI PQ200 Federal Reference Method high-volume filter samplers. Tandem samplers with PM_{10} inlets were used at both Site 1 and Site 2, with one collecting mass on a Teflon filter and the other collecting mass on a quartz filter. This enabled subsequent analysis for organic material (quartz) and silicates (Teflon) along with other elements. The filter sampling was done for 12 hr starting a 07:30 local time to characterize airborne particulate composition during the daytime when fugitive dust impacts were most likely to occur.

Sites 2 and 3 were located 227 m and 283 m at a compass direction of about 17° from the center of a circle roughly encompassing the active fly ash deposal area. Site 2 was 23 m from the dirt road (called the “berm” road) that was the source of most of the road dust impacts recorded during the study. The base of the dirt road was about 3.7 m above the elevation of Site 2 but the BAMs sampling inlets were 2.4 m above ground, placing the particulate measurements at just over 1 m from the vertical center height of road dust plumes. A seldom-used gravel “access” road was between the berm road and Site 2. The access road was 3.5 m from Site 2 and at the same elevation.

The digital camera used was a Mobotix M24M high resolution surveillance system. The primary benefit of this video system is its relatively high resolution (3 megapixels per image) and wireless capability. The camera was configured to operate Monday through Friday, from 06:30 am to 16:00 pm and coincided with the schedule of the ash handling crews. The camera viewing angle covered the northwest part of the ash pile while the image foreground included the access road, berm road and a perpendicular road that connects the berm and main roads. Six video motion windows (VMW) were defined to closely monitor activities occurring inside the camera field of view. When one or more VMWs detected movement the camera automatically stored images at a predetermined minimum frequency. The images provided a vehicle census during the study, a record of vehicular activities (i.e., grading work) and a means of quantifying vehicle speed. The types of vehicles involved in fly ash hauling and dumping were heavy duty haul trucks, water trucks, and excavators. Vehicles involved in road and drainage constructions included front loaders, graders, bulldozers, a watering truck, a school

bus (for personnel transport), pickup trucks and small utility vehicles of various types. The surveillance system helped determine the likely cause of observed light scattering spikes at Site 2.

Fly Ash Plume Modeling

The EPA AERMOD atmospheric dispersion model (EPA, 2004) is the tool that is recommended by the EPA for computing the dispersion of atmospheric pollutants within a few tens of kilometers from a regulated source. AERMOD is capable of simulating pollutants emitted from a non-buoyant area source such as a fly ash disposal site. AERMOD is a Gaussian plume model with the highest simulated pollutant concentrations at plume centerline and decreasing concentrations--following a Gaussian distribution--toward a plume's lateral (cross-wind) boundaries. AERMOD is a spatially-uniform steady-state model in that it only considers one set of meteorological conditions for representing the entire period of pollutant transport from source to downwind receptor. The model calculates a pollutant concentration C based on a user-supplied emission rate Q . If AERMOD is run with $Q=1$ then each simulated concentration is mathematically equivalent to the rate-normalized concentration C/Q because in the model C is directly proportional to Q .

The Gaussian plume assumption represents an analytical challenge because it is a statistical approach to dispersion modeling that is most relevant when simulating a large number of plumes under similar conditions. In truth, no plume is "infinitely" wide as the Gaussian assumption implies. When used in the current analysis an extremely wide plume can yield non-zero estimates of C/Q at downwind monitoring sites. These results would produce very high emission rates but with a corresponding very low probability of being real. To avoid this problem, all AERMOD model results were based on a $4\sigma_y$ finite-width plume rather than allowing AERMOD to assume a Gaussian plume of infinite width. Thus, the value of C/Q was set to zero for periods when a receptor (i.e., air monitoring station) was more than $2\sigma_y$ from the plume centerline.

AERMOD is normally run using hourly meteorological data. This approach neglects sub-hourly meteorological variability that could be important in determining one hour average concentrations. Wind direction variations are especially problematic in summer when wind speeds are often light and direction variability is large. This problem was minimized by processing six individual 10-min meteorological averaging periods each hour and using them to model 10-min average concentrations that were subsequently combined to yield hourly averages.

The method used here was to provide AERMOD all meteorological parameters that were measured at the study site and allow the model to select the parameters using its built-in data preferences. Thus, AERMOD was given wind speed, direction (θ), air temperature, relative humidity, the standard deviation of the vertical wind component (σ_w) and the standard deviation of the horizontal wind direction (σ_θ) at both tower levels along with solar radiation, net radiation, precipitation amount and surface roughness (z_θ). Surface roughness--computed by wind direction sector for the study site using data for 10-min periods under neutral atmospheric stability--averaged 0.03 m for the important southerly sectors. This low value indicates a relatively smooth surface. Wind speed, wind direction, σ_w and σ_θ are the parameters most likely to be used by AERMOD when calculating C/Q . AERMOD also reads and uses other derived parameters (e.g., surface heat flux, Monin-Obukhov length). These were computed following procedures outlined in AERMOD documentation (EPA, 2004) but were unlikely to be used. The height of the mixing layer (z_m) was not measured onsite. A constant 800 m was used as the convective z_m for all events and a constant 200 m was input for the mechanically-mixed z_m . Tests conducted on sensitivity to z_m in AERMOD found that the value did not affect C/Q over the very short distances between the source (flyash disposal site) and the monitoring sites. Thus, the parameters that controlled simulated C/Q in this study were measured U , θ , σ_θ and σ_w .

AERMOD was applied in two ways to simulate dispersion from an area source with a diameter of 7 m and a release height of zero. First, simulations were based on actual sub-hourly meteorological data and results combined to produce one hour average C/Q for four alternate source locations on the

dry stack. These locations were at the downwind, upwind, western-most and eastern-most edges of the circle defining the active ash storage area (see Figure 2). This approach provided estimates of the uncertainty due to not knowing the exact location of ash deposits for each event hour. A second method applied a Monte Carlo sampling procedure to estimate alternate sub-hourly meteorology based on measured variations in input parameters. This approach provided estimates of the uncertainty due to meteorological variability between the monitoring and ash disposal sites. In both approaches, the area emission rate for the i th particle size fraction was determined from

$$\text{Equation (5)} \quad Q_a(i) = \frac{C_{xs}(i)}{(C/Q)}$$

with units of emitted particle mass per unit area per unit time. The value $C_{xs}(i)$ represents the “excess” concentration associated with the fly ash fugitive dust plume and derived from observations as described later. During each hour the mass of fly ash processed at the source was known (M_{ash}) in units of mass of ash per unit area per unit time. The equivalent particulate emission factor $E_{ash}(i)$ --with units of emitted particle mass per mass of processed ash--was computed as

$$\text{Equation (6)} \quad E_{ash}(i) = \frac{Q_a(i)}{M_{ash}} .$$

Deriving Road Dust Emissions

Vehicles traveling on two unpaved roads near Site 2 produced dust plumes that were sampled and used to compute fugitive road EFs. Vehicle movement on unpaved surfaces was expected to be a major contributor to fugitive emissions during fly ash handling at the dry stack. Thus, the road emissions presented an opportunity to test existing unpaved road EFs. Both roads were oriented northwest-southeast just south of the open field where all but the background study instrumentation was operated (Figure 2). The roads were straight and level. The busiest road--denoted the “berm” road--was covered in compacted clay. This road was resurfaced beginning in May and worked continued into June. In early June the road was soft and prone to relatively high fugitive particulate emissions because of the dry, uncompacted nature of its surface. After June, traffic and frequent watering for dust suppression further compacted the clay surface and minimized emissions. By early August the surface was harder and emissions were visibly less.

A second “access” road was located at the same elevation as Site 2. This road, composed of small- and medium-size limestone gravel overlaying compacted soil, rarely experienced vehicular traffic and was never watered. However, traffic on it tended to drive faster than on the berm road. In addition, fugitive dust emissions from the access road were usually more visible than emissions from the berm road once the latter had become compacted.

Meteorological data were screened to identify hours when airflow conditions were favorable for blowing dust from the nearby roads toward the monitors at Site 2. Although Site 3 measurements detected elevated hourly particle concentrations associated with fugitive road dust, the data could not be used to estimate fugitive emission rates because no nephelometer data were available at the site to characterize the rapid evolution of the brief events.

Hours that were meteorologically favorable for detecting fugitive road dust emissions were further screened using camera images. These images allowed identification of events when vehicles passed Site 2 on the berm or access road, the type of vehicle and its approximate speed. Vehicle passages were matched with b_{scat} spikes. In some cases no spikes were detected. In other cases, b_{scat} variations that had the appearance of spikes caused by “local” sources were found to be associated with activity other than passing vehicles (e.g., excavation, grading and mowing). An analysis of these spikes indicated that nearly all vehicular and other major fugitive sources increased b_{scat} above baseline values by 50 to several hundred percent per event. Thus, we defined a local source impact as occurring during any 5-min period when 1-min b_{scat} peaked >20 percent above baseline values measured during the

minutes before and after the spike. Smaller spikes were ignored. Generally, when there was no visible activity occurring near Site 2 the b_{scat} time trace exhibited very little variation.

There were several b_{scat} events for which no explanation was evident from camera images. Some of these events occurred when activity was visible at the fly ash storage site but rarely were the wind directions favorable for transporting particles from there toward Site 2. Short-term b_{scat} spikes were rarely associated with fly ash disposal activity and this was expected due to the much greater transport distances involved and the lower emission rates expected. Unexplained events were not characterized and their cause is unknown.

Forty-two camera-identified vehicle passages were unambiguously associated with favorable airflow. Of these, 36 were on the berm road and 6 on the access road. A visual census of vehicles passing Site 2 provided the basis for the road dust analysis. The foundation of this determination is due to Hanna et al. (1982) who give the following equation for calculating concentrations of an airborne pollutant downwind of a ground-level line source:

$$\text{Equation (7)} \quad C = \frac{Q_l}{1.23 U} \left(\frac{U}{4 K_z x} \right)^{1/2} \exp \left(- \frac{U z^2}{4 K_z x} \right) .$$

In equation (7), Q_l is the road emission rate (mass emitted per unit length of road per unit time), x is the distance traveled from the point of emission to the point of measurement and z is the vertical distance between plume centerline and the concentration location. This steady-state equation, based on similarity theory, assumes that the vertical diffusion of a pollutant can be characterized by vertical eddy diffusivity K_z . Implicit in using K_z is the assumption that the dispersive eddies are small compared to vertical plume dimensions, an assumption that is most valid for a ground-level plume. Equation (7) combined with field measurements were used to derive a ‘‘puff’’ emission rate ΔQ_l from derived quantity ΔC .

Once the emission rate is known the unpaved road EF (E_{road}) is computed as

$$\text{Equation (8)} \quad E_{road} = \Delta Q_l \Delta t$$

for a road dust puff lifetime of Δt .

Separating Road Dust and Fly Ash from Background Particulate Levels

Individually quantifying road and fly ash disposal contributions to measured hourly $C_{PM2.5}$ and C_{PMc} ($=C_{PM10} - C_{PM2.5}$) was difficult because there is no direct means of knowing the degree to which airborne particles were derived from soil or fly ash (soil and ash chemical signatures are too similar). We used an indirect phenomenological approach based on camera information, measured b_{scat} and derived statistical relationships between various measured parameters. This method was not perfect but it captured the majority of local sources and enabled us to isolate those events that were most likely associated only with fugitive fly ash emissions. If anything, the approach may have enabled some contributions from unknown sources to impact the fly ash calculations thereby slightly overestimating fly ash fugitive emissions.

Particle concentrations for the two mass fractions at Sites 2 and 3 were impacted by background sources (i.e., upwind of the plant site), fly ash disposal activity and local sources (those between the fly ash site and the monitoring sites). Measured background levels of PM_{10} and $PM_{2.5}$ when airflow was from the southerly directions were provided by Site 1 data. Subtracting background values from Site 2 and 3 values provided concentrations due to the combined effects from fly ash disposal and local sources. The fly ash contribution to measurements at Sites 2 and 3 were computed using measured b_{scat} at Site 2 to remove local source contributions. The procedure was developed after analyzing 447 hr of data when wind directions were from the south-southeast through south-southwest sectors. Relationships were examined between b_{scat} , $C_{PM2.5}$, C_{PMc} and associated meteorological parameters.

From scaling arguments it can be shown that, unless the number of particles in the PM_c size fraction is a lot more abundant than those $<2.5 \mu m$, the measurement of b_{scat} will be more sensitive to $C_{PM2.5}$ than C_{PMc} . Note that $C_{PM2.5}$ is significantly correlated (>99 percent confidence) with C_{PMc} but the

associated variance (r^2) is small, ~10 percent. This implies that a portion of the $PM_{2.5}$ and PM_c at Site 2 comes from the same source(s) but also that about 90 percent of the variability in both is independent. Multivariate analysis for conditions when airflow was from the south-southeast through west southwest sectors also yielded the following:

- b_{scat} is significantly correlated with Site 2 $C_{PM_{2.5}}$ and C_{PM_c} but the association with C_{PM_c} is weak (i.e., they share little variance in common). The correlation of b_{scat} with C_{PM_c} is due to the association between $C_{PM_{2.5}}$ and C_{PM_c} .
- Seventy-six percent of the variance in $C_{PM_{2.5}}$ at Site 2 is associated with variance in b_{scat} and a small additional amount of variance is associated with relative humidity at 2.3 m (f_2) and the standard deviation of b_{scat} ($\sigma_{b_{scat}}$). Predictor variable confidence exceeds 99 percent for all predictors.
- The multivariate regression between $C_{PM_{2.5}}$ and its predictors b_{scat} , $\sigma_{b_{scat}}$ and f_2 ($r^2=0.81$) is given by

Equation (9)
$$C_{PM_{2.5}} = c_{b_{scat}}b_{scat} + c_{f_2}f_2 + c_{\sigma} \sigma_{b_{scat}} + c_{int} .$$

In equation (9), $c_{b_{scat}} = 0.201 \text{ Mm } \mu\text{g m}^{-3}$, $c_{f_2} = -0.054 \mu\text{g m}^{-3} \text{ percent}^{-1}$, $c_{\sigma} = 0.052 \text{ Mm } \mu\text{g m}^{-3}$ and $c_{int} = 6.56 \mu\text{g m}^{-3}$. This equation provides a means for directly estimating $C_{PM_{2.5}}$ from other measured parameters. The unexpected association between $C_{PM_{2.5}}$ and $\sigma_{b_{scat}}$ was not nearly as strong as the association between C_{PM_c} and $\sigma_{b_{scat}}$.

The larger particles in the coarse size fraction are not well represented by visual wavelength b_{scat} primarily because of the lower light scattering efficiency and smaller number concentration of particles larger than a couple micrometers (Friedlander, 2000). However, it is clear from examining b_{scat} and C_{PM_c} time series plots that fugitive sources produce coarse particles. One way to model C_{PM_c} is to find a surrogate for the various physical processes (vehicle passages, ash dumps, etc.) that generate fugitive emissions. We found the best surrogate to be the standard deviation of 1-min b_{scat} . Peaks in b_{scat} are an indication of physical activity that generates fugitive dust. As the activity increases and produces more PM_c , 1-min b_{scat} exhibits more peaks and these translate into larger variance in b_{scat} .

A multivariate analysis of C_{PM_c} and various parameters yielded the following:

- Hourly C_{PM_c} is highly correlated ($r^2 = 0.67$) with $\sigma_{b_{scat}}$.
- C_{PM_c} is significantly correlated with wind speed at 2.3 m (U_2).
- $C_{PM_{2.5}}$ provides some additional correlation with C_{PM_c} beyond what is captured by $\sigma_{b_{scat}}$ and U_2 .
- Jointly, $\sigma_{b_{scat}}$, U_2 and $C_{PM_{2.5}}$ are associated with 71 percent of the variance in C_{PM_c} . Although somewhat lower than the model of $C_{PM_{2.5}}$, this is still a very high correlation. The resultant model is expressed as

Equation (10)
$$C_{PM_c} = c_{\sigma} \sigma_{b_{scat}} + c_{U_2} U_2 + c_{PM_{2.5}} C_{PM_{2.5}} + c_{int} .$$

In equation (10), $c_{\sigma} = 3.87 \text{ Mm } \mu\text{g m}^{-3}$, $c_{U_2} = 7.85 \mu\text{g s m}^{-4}$, $c_{PM_{2.5}} = 1.57$ and $c_{int} = -29.4 \mu\text{g m}^{-3}$. All predictors in equation (10) are significant at greater than 99 percent confidence. Comparing equations (9) and (10) regression parameters reveals that C_{PM_c} is more than ten times more sensitive to $\sigma_{b_{scat}}$ than $C_{PM_{2.5}}$ is to b_{scat} .

Given these statistical relationships, it is possible to estimate $C_{PM_{2.5}}$ and C_{PM_c} from other parameters that are continuously measured onsite. The procedure to determine fugitive dust plume hourly “excess” concentrations for the i th particle size fraction at Site 2 was to first compute an adjusted concentration that removed the influence of local sources from the measured value, $C_{obs}(i)$:

Equation (11)
$$C_{adj}(i) = C_{obs}(i) - C_{local}(i) .$$

In equation (11),

$$C_{local}(i) = c_{b_{scat}}(i)(b_{scat}^{obs} - b_{scat}^{adj}) + c_{\sigma}(i)(\sigma_{b_{scat}}^{obs} - \sigma_{b_{scat}}^{adj}) + c_{PM_{2.5}}(i)(C_{PM_{2.5}}^{obs} - C_{PM_{2.5}}^{adj})$$

where “obs” and “adj” superscripts refer to the hourly values measured, respectively, across all minutes and those minutes for which no local disturbance were identified. Minutes impacted by a local source were those when b_{scat} increased >20 percent above the baseline value. Note that $c_{b_{scat}}=0$ for the PM_c

size fraction and $c_{PM_{2.5}}=0$ for the $PM_{2.5}$ size fraction. In addition, $C_{PM_{2.5}}$ must be computed before C_{PM_c} because the former is needed to compute the latter.

$C_{xs}(i)$ is computed from $C_{adj}(i)$ as

$$\text{Equation (12)} \quad C_{xs}(i) = C_{adj}(i) - C_{bck}(i)$$

with $C_{bck}(i)$ representing the Site 1 background concentration of particle size fraction i . Site 3 measurements were immediately downwind of Site 2 when winds were favorable for fugitive fly ash impacts. Adjusted Site 3 concentrations were computed assuming equal proportionality between Site 3 and Site 2 such that the ratio of C_{adj}/C_{obs} was equal at the two sites.

RESULTS

Fly Ash Emission Factors

Hours were analyzed for fugitive fly ash emissions as long as they met a list of criteria that included wind directions between south-southeast and south-southwest (to ensure optimal alignment between the source area and downwind monitors), the availability of valid data, no precipitation, the absence of other dust source interferences whose influence could not be removed (including screening of events based on PM_{10} chemical signatures to remove periods clearly affected by biomass burning), and a *reliable* indication that fly ash disposal was actively occurring. Hourly fly ash disposal activity was determined using camera imagery and information from the daily ash handling logs.

After removing background and local source interferences, measured particulate concentrations were, in some cases, not significantly different from zero. Measurement sensitivity was determined prior to the start of ambient measurements following manufacturer guidelines that all instruments be initially operated for 3 days with special inlet filters that remove most particles smaller than $10 \mu\text{m}$ in size. A subsequent comparison of the “zero” concentration data provides information on measurement sensitivity. Note that instruments can output negative values when the detection signal is low because the output voltage generated when scanning an exposed segment of filter tape is compared to a reference voltage generated by scanning a clean tape segment. Our zero-air comparisons yielded a mean sensitivity for the BAMs data of $\pm 3.6 \mu\text{g m}^{-3}$ for both PM_{10} and $PM_{2.5}$ measurements. Figure 3 illustrates the frequency distributions of C_{obs} at each measurement site during the periods when ash was typically processed. Fine particle concentrations rarely exceeded $30 \mu\text{g m}^{-3}$ but PM_{10} values exceeded $60 \mu\text{g m}^{-3}$ a significant fraction of the time. Mean measured values (\bar{C}), listed in each plot, do not vary much by site for $PM_{2.5}$ but exhibit a lot of differentiation for PM_{10} . This shows that fugitive dust emissions are primarily in the coarse particle size fraction. Figure 4 illustrates the distributions of $PM_{2.5}$ and PM_c C_{xs} for the cases analyzed to determine EFs. About 60 percent of the $PM_{2.5}$ C_{xs} and 47 percent of the PM_c C_{xs} was below $3.6 \mu\text{g m}^{-3}$ making the signal-to-noise ratio especially high for $PM_{2.5}$ emissions.

Given this knowledge it is somewhat surprising that background levels of $PM_{2.5}$ and PM_c were seldom greater than levels measured at Sites 2 and 3. Perhaps it is a testament to the significance of fugitive dust emissions that, even after correcting for local source impacts, the downwind particulate measurements were almost always above background during the daytime when fly ash disposal was active. Though C_{xs} values were not always $> 3.6 \mu\text{g m}^{-3}$ they were usually $> 1 \mu\text{g m}^{-3}$ (BAM precision level). However, when C_{xs} was $< 1 \mu\text{g m}^{-3}$ it was usually $<< 1 \mu\text{g m}^{-3}$ (and even < 0). For cases when $-4 \mu\text{g m}^{-3} < C_{xs} < 0.5 \mu\text{g m}^{-3}$, C_{xs} was arbitrarily set to $3.6 \mu\text{g m}^{-3}$ to calculate an EF upper limit during extremely low and highly uncertain plume levels (cases were not analyzed if $C_{xs} < -4 \mu\text{g m}^{-3}$). These were typically events when ash handling rates were very low at the disposal site. Table 1 summarizes the EFs computed from field data and compares them with values derived using aggregate AP-42 EF formulations for ash handling processes [i.e., equations (2) and (3)]. These results include only those hourly events when the derived number of ash truck loads was at least one and when EFs were computable using both the field study and AP-42 methods.

Emission factors based on field study data exhibited a much larger range than factors derived from AP-42 formulations. This is probably because natural variability in atmospheric conditions coupled with large variations in ash handling conditions conspired to produce large variations in downwind concentrations used to compute fugitive fly ash EFs. Factors derived using AP-42 formulations were based on a small range in input parameters and the EFs themselves do not rely on downwind measurements for verification. In addition to differences in range/variability, field study EFs were smaller in magnitude and more strongly skewed toward low values than AP-42 values (and this was despite the fact that EFs based on field study data included values representing an upper limit whenever extremely low concentrations were measured). Coarse mass EFs averaged 80 percent less for field study data compared to AP-42 values and $PM_{2.5}$ EFs averaged 34 percent less. Median values showed an even greater disparity. This is especially noteworthy because of the conservative approach used to estimate EFs when C_{xs} was very low.

Emission Factor Uncertainties

Simulated emission rate uncertainty (which translates directly into EF uncertainty) was examined by computing the variability in AERMOD-derived Q_a due to uncertainty in the exact location of fugitive emissions on the fly ash dry stack and uncertainty in the meteorological data input to AERMOD. The Q_a uncertainty due to source location (“location” uncertainty) derives from the fact that the exact distance and direction from where ash was deposited relative to the downwind monitors was not known during any given hour. Source-receptor distances varied from 176 to 278 m for Site 2 and from 232 m to 334 for Site 3. Likewise, source-receptor directions varied $\pm 12^\circ$ relative to direct alignment between the assumed fly ash emission centroid at Sites 2 and 3. Meteorological uncertainty exists because meteorological measurements critical to AERMOD dispersion calculations were co-located with the downwind monitors somewhat removed from the source. In a convective boundary layer turbulence and its impact on winds can vary considerably over the few hundred meters separating the source and measurement locations especially when using 10-min averaging periods for dispersion calculations.

Location uncertainty was determined by simulating downwind impacts for four separate locations representing extremes in source-receptor distance and direction (see locations in Figure 2). The resulting emission rates are denoted Q_{loc} . Meteorological uncertainty was examined using a Monte Carlo re-sampling of sub-hourly meteorological parameters for each fugitive fly ash event. Rates generated from this exercise are denoted Q_{met} . The source position was set to the ash disposal centroid location (source-receptor distances of 227 and 283 m for Sites 2 and 3) for Q_{met} simulations. A thousand independent replications of 10-min meteorological parameters provided alternate realities of conditions driving transport and diffusion. Meteorological variances were taken directly from the observed variability of 10-min parameters during each event hour. Each replicated set of meteorology was modeled by AERMOD. The means and uncertainties associated with Q_{met} represent an independent calculation of the sensitivity of simulated emission rates to meteorological variability between the measurement location (tower) and the fly ash disposal area. Wind direction variability can result in either direct plume hits on a receptor, a “glancing blow” by a plume or a total miss. Impacts from plumes that passed a receptor at a distance $>2\sigma_y$ were assumed to make no contribution to measured particle concentrations. However, plumes that impacted a receptor “on-edge” (near the $2\sigma_y$ limit) can result in high emission rate estimates and contributed to the large upper tail of the Q_{met} (and E_{ash}) frequency distributions.

Simulated 90 percent confidence intervals for Q_{loc} and Q_{met} are summarized in Table 2. Meteorological uncertainty effects were larger than location uncertainty effects. Source location uncertainty is more likely to produce emission rate estimates that are less than the average rate based on all four potential source locations. Meteorological uncertainty is more likely to produce overestimates compared to the average of Q_a based on all meteorological realizations. The upper distribution tail is so extreme that mean Q_{met} values in Table 2 are based only on the results that fall within the 90 percent

confidence interval to avoid an otherwise absurdly large summary statistic. The mean for coarse mass Q_{met} was 34 percent higher than the mean for Q_{loc} (denoted \bar{Q}_{loc}) but the fine mass mean Q_{met} was nearly double \bar{Q}_{loc} . Note that $Q_a = \bar{Q}_{loc}$ when calculating E_{ash} (preceding section) in order to account for the known source location uncertainty.

These results should not be interpreted as indicating that the Q_{met} results are somehow more realistic than Q_{loc} because the former only represent *hypothetical* multi-parameter variations in meteorology. Q_{met} results indicate the level of uncertainty that would exist if the observed meteorological data did not represent conditions over the ash disposal area. The rationale for examining this issue is based on the elevation difference between the top of the dry stack and the tower measurements and the distance separating the tower from the source area. The dry stack top is 20-30 m above the elevation at Site 2 and 17-27 m above the top measurement level on the meteorological tower. Although the slope from the dry stack to the field is relatively smooth and the assumption is reasonable that airflow streamlines are terrain-following (especially likely due to the low wind speeds involved), there is always the chance that elevation differences and distance might conspire to introduce meteorological dissimilarities between the tower and the dry stack. Thus, the Monte Carlo test for meteorological uncertainty is an acknowledgement of its potential impact on emission rate estimates while recognizing that test results are expected to overstate the influence of any differences on simulated dispersion results.

The $PM_c E_{ash}$ values based on this study are so much lower than the AP-42 based values that the potential meteorological uncertainty does not alter the conclusion that the former are significantly lower than the latter. The difference between the *mean* study-derived and AP-42 $PM_{2.5} E_{ash}$ values is less than that for $PM_c E_{ash}$ and the two sets of $PM_{2.5}$ results may not be as different as implied based on the potential for meteorological uncertainty. However, the *median* $PM_{2.5} E_{ash}$ values still exhibit a large difference that remains significant even if meteorological uncertainty was important.

Unpaved Road Dust EFs

The differences between AP-42 and our estimates of E_{ash} are due entirely to the AP-42 estimates of fugitive dust from vehicles driving over ash at the disposal site [equation (3)]. This is because the average contribution to total fugitive fly ash emissions of grading operations is >99 percent of the total computed emissions using the AP-42 formulations. This section reviews the problem with these estimates.

The AP-42 methodology is not without its problems. The vehicle (grader) weight is known reasonably well as is the amount of ash processed per load and the number of loads processed per hour. However, ash moisture content (M) is a design value supplied by engineers familiar with the process. The actual value of M in equation (2)--and its absence from equation (3)--is a potential source of error. The design of the ash handling system calls for a range in M of 10-20 percent. Equation 2 is based on data for $M < 5$ percent and silt content $S < 20$ percent. Likewise, equation (3) is based on data when $M < 13$ percent and $S < 25$ percent. Silt content of fly ash is near 100 percent. Factoring in error introduced by selecting wind speed (i.e., which tower level to use), distance traveled by the grading equipment and in the speed of moving vehicles [the grader speed of ~ 5 mi hr⁻¹/11 km hr⁻¹ is at the lower limit of the data used to develop equation (3)] it is easy to understand how the AP-42 approach may not perform that well for this particular operation. A series of different AP-42 based E_{ash} values were computed to account for modest uncertainties in inputs, specifically M (10-20 percent), S (± 10 percent error), distance traveled (± 20 percent error) and wind speed (based on two tower level options). The mean of the AP-42 $PM_c E_{ash}$ values that included parameter uncertainty was nearly identical to that listed in Table 1 but the range expanded to 156-443 g Mg⁻¹, the median increased to 242 g Mg⁻¹ and the standard deviation increased to 62 g Mg⁻¹. These results illustrate that uncertainty inherent in the AP-42 approach is capable of producing greater variability in E_{ash} than is implied by using single values for the

input parameters. However, it is unlikely that the AP-42 method can produce significantly lower values (i.e., more in line with those computed using our approach).

Fugitive road dust EFs were not an original focus of this study but presented an opportunistic analysis because of the presence of unpaved roads and vehicular traffic just south of Site 2. The methodology used here is similar to that described by Cowherd et al. (1974). In their scheme an atmospheric particle sampler is located downwind of a straight road. The sampler collects particles while vehicles travel down the road. The road dust plume represents emissions from a semi-continuous “infinite” line source. Measured particle concentrations (or deposition amounts using dustfall collectors) are then used together with estimates of vertical diffusion rates and observed wind speed to calculate the line source emission rate needed to produce the observed particle levels.

In our study the line source is instantaneous rather than semi-continuous but the principle is the same. The primary difference is that when earlier studies were done researchers relied on long exposure times so that sufficient particle samples could be collected to recover a viable measurement. However, the present analysis relied on a fast-response nephelometer to measure the passage and intensity of brief fugitive dust plumes and statistical relationships between measured b_{scat} and meteorological parameters enabled a calculation of particulate concentrations (and hence, emission factors) from b_{scat} . The need to have 1-min b_{scat} data precluded using Site 3 particulate concentration data for this work.

The analysis was performed using a formula derived from equation (7) with 1-min wind speed, wind direction and σ_w data together with b_{scat} . Calculations require K_z , U , x and ΔC (the dust concentration spike association with a passing vehicle). The only road dust events analyzed were those occurring when there was clearly a vehicle associated with a b_{scat} spike and winds at both tower levels were blowing from the south-southeast through west sectors. The distance between the point of origin of the plume and the monitoring site was computed as

$$x = x_{\perp} / \cos(\theta_r)$$

with x_{\perp} representing the perpendicular distance of Site 2 from the berm or access road and θ_r representing the angular difference between wind direction and 225° (the direction perpendicular to the road). The transport time from road to monitoring site and K_z determined the expected plume depth as it passed over the site. This in turn determined the most appropriate tower data to use to calculate dispersion. Very shallow plumes would be best represented by data from 2.3 m. Most plumes, however, were so deep that interpolating between the tower levels was a better choice. Thus, two plume depths and two transport distances were determined for each event using data from the two tower levels. Plume depth $D_p = 2\sigma_z$ was initially estimated as the average depth computed from data at the two levels where σ_z was the vertical plume dispersion coefficient calculated following the formulation in AERMOD for non-buoyant plumes in an unstable boundary layer (Cimorelli et al., 2004):

$$\sigma_z = \frac{0.6025 x \sigma_w}{U} .$$

Comparing $\frac{1}{2}D_p$ with the two tower measurement heights determined what data to use for computing the final values of θ_r , K_z , U , x : 2.3-m data when $\frac{1}{2}D_p \leq 2.3$ m, vertically interpolated (linear) data when 2.3 m $< \frac{1}{2}D_p < 9.6$ m, and 9.6-m data when $\frac{1}{2}D_p \geq 9.6$ m. Table 3 lists the average inputs and plume parameters for analyzed road dust events.

Results of the E_{road} analysis based on observed concentrations and the estimated particle dispersion formulation represented by eq 7 are summarized in Table 4. Coarse mass E_{road} --denoted $E_{road}^{ob}(PM_c)$ --was found to average 90 g per vehicle kilometer traveled (VKT^{-1}) for both roads but with emissions from the access road averaging nearly 4 times greater than the berm road. Individual event values ranged from near zero to over 600 g VKT^{-1} . However, the distribution of $E_{road}^{ob}(PM_c)$ is skewed toward small values with a median emission factor of 44 g VKT^{-1} . Values of $E_{road}^{ob}(PM_{2.5})$ are much smaller, averaging 4 g VKT^{-1} with a median of around 2 g VKT^{-1} .

Emission factors computed using AP-42 formulations are summarized in Table 4 for the same events. AP-42 provides two methods as previously described (E_{ir} and E_{pr}). Less traffic at industrial

sites is expected to contribute to higher levels of surface silt (granular material smaller than 75 μm in size). Also, industrial site traffic is expected to move more slowly such that vehicle speed is unlikely to be important. Intermittent precipitation can be expected to condition public road surfaces in ways not expected for industrial roads (unless the latter are watered as is now standard practice at many industrial sites). This leads to the use of surface moisture content when estimating E_{pr} .

Averages of road surface parameters and estimated EFs are listed in Table 4 for the 42 road emission events analyzed. Field data indicated that the access road EFs were higher than those for the berm road, consistent with the public road formula but not the industrial road formula. All methodologies agree that $\text{PM}_{2.5}$ EFs are much lower than PM_c EFs. Also, E_{road}^{ob} was less than E_{ir} and E_{pr} for both roads. The large differences between E_{road}^{ob} and E_{ir} are the likely reason why our derived values of E_{ash} are so much lower than their AP-42 counterparts.

CONCLUSIONS

Five months of measurements at the TVA Colbert fossil plant captured a number of hours when meteorological conditions coincided with activities that produced fugitive particulate emissions. A methodology for removing local source effects on measured particle concentrations enabled an estimate of fly ash fugitive particulate emission rates and emission factors. A separate set of brief (~1-3 min) periods was analyzed to independently estimate fugitive road dust emission factors. Results from both source types were compared with EFs derived using formulations in the EPA AP-42 emissions handbook.

The fly ash disposal process at Colbert requires that “dry” ash (although the ash is not totally free of water this process is distinctly different from the “wet” process in which ash is pumped in a water slurry to a wet ash disposal pond) be dumped from the bed of a haul truck and then immediately spread into a layer of uniform thickness before the next load arrives. Multiple ash loads are usually deposited during peak work hours. Downwind measurements of hourly particle concentrations appear to respond as expected to this activity. However, atmospheric variability drives plume dynamics in a way that makes it difficult to measure fugitive plumes on a consistent basis. Also, during the field study some events produced such low downwind concentrations that fugitive fly ash plumes could not be detected with high confidence above the background levels. This is due in part to atmospheric variability and in part to the measurement sensitivity of the monitoring equipment. Previous studies of this type relied on even coarser measurement methods (dustfall collectors and high volume particle samples operated for extended periods of time very near the source). It is difficult to conduct close-proximity measurements in an operational setting such as the one at Colbert. To our knowledge this study represents the first attempt to conduct a fugitive dust measurement campaign at an operating fly ash disposal area. The study data integrate emissions over the multiple operations involved in fly ash disposal rather than relying on parameterizations of individual processes (i.e., dumping and grading). In addition, this study measured both coarse and fine particle at one hour time resolution thereby minimizing the uncertainties introduced when longer averaging times are involved and even more atmospheric variability comes into play. Data from this study represent a fresh examination of the fugitive emissions formulations that have been used for several decades without being re-evaluated.

The picture that emerges is that AP-42 formulations produce EFs significantly higher than those derived from the current study. When applied to ash disposal the AP-42 formulations result in a narrow range of EFs, even when the uncertainty of factors like ash moisture content and the representativeness of the formulations for high silt content materials (such as fly ash) are considered. By contrast, the natural variability of the atmosphere produces EFs that cover a much wider range of values with most clustered in the lower range of values but a few spread out to form a long upper tail to the distribution. The selection of a “best” metric is perhaps debatable under these circumstances but given that EFs are typically applied to produce long-term (especially annual) estimates of total emission it seems that use of a mean or median value is appropriate. The mean is more conservative than the median due to the

distribution skewness, but even so the EFs derived here remain quite low when compared to equivalent AP-42 EFs.

It is important to remember that EFs for fly ash disposal are strongly influenced by the AP-42 formulation [equation (3)] for fugitive emissions from vehicles moving over unpaved surfaces. This formulation is distinctly different from the one recommended for use on unpaved public roads [equation (4)] in which vehicle speed and surface moisture content is treated explicitly. Thus, the comparison of fugitive road EFs from both AP-42 and field data confirms our belief that the AP-42 industrial unpaved road EF formulation is biased high for a surface composed mostly of silt-sized particles. Results from this study suggest that coarse particle EFs for unpaved surfaces are much less than those derived using either the industrial or public road formulation. Fine particle ($PM_{2.5}$) EFs determined by the present study are also somewhat lower than those produced using either AP-42 formulation.

Reasons why EFs derived from AP-42 formulations are greater than those derived by this study are not obvious but a number of reasons can be contemplated. The EF formulation for dropping operations is based on materials that were far drier than the moisture content of the fly ash. The EF for vehicles driving on unpaved surfaces at industrial sites was based on data for surfaces with silt content far below what is appropriate for fly ash and most data were for vehicles traveling at speeds well above those involved in grading fly ash. Contemporary measurement technology is capable of providing hourly particle concentrations whereas older measurements utilized high-volume filter measurements that required sampling periods longer than one hour and were incapable of detecting short-term emission rate variations. Long sampling periods necessarily include variable meteorology and that implies the possibility of a highly variable relationship between emissions source and downwind measurement locations while measurements are made. It is not clear how this might affect derived emission factors but it is not surprising that AP-42 formulations provide emission estimates that do not match closely with those measured using modern techniques.

Finally, it is interesting to compare the relationship between $PM_{2.5}$ and PM_{10} for the different sources and emission factor derivations. The ratio of $PM_{2.5}$ to PM_{10} in fugitive fly ash plumes was observed to be 9 percent which compares very well with the ratio of 10 percent that is inherent in the AP-42 formulations. However, the fraction of PM_{10} that is $PM_{2.5}$ in fugitive road dust was observed to be only 4 percent which is considerably lower than the 10 percent ratio in the AP-42 results. The ratio of $PM_{2.5}/PM_{10}$ of 0.1 in the AP-42 EFs is consistent with the ratio reported by a fugitive dust study of western sources (WRAP, 2005). That same report also mentioned that there was some evidence the ratio might be closer to 0.05 and that would be very similar to the 0.04 ratio reported here.

REFERENCES

Cimorelli, A.J.; Perry, S.G.; Venkatram, A.; Weil, J.C.; Paine, R.J.; Wilson, R.B.; Lee, R.F.; Peters, W.D.; Brode, R.W.; Paumier, J.O. *AERMOD: Description of Model Formulation*, U.S. Environmental Protection Agency, Research Triangle Park, NC, 2004, EPA-454/R-03-004.

Code of Federal Regulations, Title 40, Sections 70.2 and 71.2, Office of the Federal Register, United States of America Government Printing Office, Washington, DC.

Cowherd, C. Jr.; Axetell, K. Jr.; Guenther, C.M.; Jutze, G.A., "Development of Emission Factors for Fugitive Dust Sources", EPA-450/3-74-037, Prepared for the U.S. Environmental Protection Agency by the Midwest Research Institute, Kansas City, MO, 1974.

Dyck, R.J.; Stukel, J.J., "Fugitive dust emissions from trucks on unpaved roads", *Env. Sci. Technol.* 1976, 10, 1046-1048.

EPA, *Compilation of Air Pollutant Emission Factors - Volume I: Stationary Point and Area Sources*, AP-42 Fifth Edition, U.S. Environmental Protection Agency, Research Triangle Park, NC, 1995 with subsequent updates.

EPA, *User's Guide for the AMS/EPA Regulatory Model - AERMOD*, EPA-454/B-03-001, U.S. Environmental Protection Agency, Research Triangle Park, NC, 2004.

Friedlander, S.K. *Smoke, Dust, and Haze*, Oxford University Press, New York, NY, 2000, pp. 130-139.

Hanna, S.R.; Briggs, G.A.; Hosker, R.P. *Handbook on Atmospheric Diffusion*, DOE/TIC-11223, U.S. Department of Energy, 1982.

Watson, J.G.; Chow, J.C.; Chen, L.; Wang, X.; Merrifield, T.M.; Fine, P.M.; Barker, K. "Measurement system evaluation for upwind/downwind sampling of fugitive dust emissions", *Aerosol and Air Quality Research* 2011, 11, doi: 10.4209/aaqr.2011.03.0028.

WRAP, "Analysis of the Fine Fraction of Particulate Matter in Fugitive Dust - Final Report", Prepared for the Western Governors' Association Western Regional Air Partnership by the Midwest Research Institute, 2005.

Table 1. Fly ash dry disposal fugitive emission factors derived from field data and using AP-42 formulations for dropping and grading operations.

Particle Size Range	Source	Number of Events	Range	Mean	Median	Standard Deviation
			(grams of particles emitted per Mg of ash)			
PM _c	Field data	74	0-658	53	9	113
PM _c	AP-42	74	173-322	260	232	40
PM _{2.5}	Field data	76	0-198	19	6	33
PM _{2.5}	AP-42	76	19-36	29	26	5

Table 2. Average simulated fugitive fly ash emission rates ($\text{g ha}^{-1} \text{ s}^{-1}$) for all event hours on days when the site material processing log indicated non-zero fly ash disposal activity.^a

Particle Size Fraction	Mean Q_{loc}	Q_{loc} Uncertainty^b (90% Confidence)	Mean Q_{met}	Q_{met} Uncertainty^c (90% Confidence)
Coarse	717	-86% to +149%	962 ^d	-61% to +1374%
Fine	84		159 ^d	-60% to +1577%

^aResults are based on the assumption of a finite-width plume equal to $\pm 2\sigma_y$. A minimum particle concentration of $0.5 \mu\text{g m}^{-3}$ was assumed.

^bDue to uncertainty using 4 different source locations.

^cDue to meteorological uncertainty.

^dExcludes values outside the 90 percent confidence interval.

Table 3. Average parameters used to compute dispersion of fugitive road dust at Site 2.

Parameter	Mean
U , m s ⁻¹	2.0
x , m	29
σ_w , m s ⁻¹	0.31
K_z , m ² s ⁻¹	0.9
Plume depth ^a , m	6

^aEquals $2\sigma_z$.

Table 4. Data, road conditions and mean fugitive road dust emission factors.^a

Method	Road	Sample Size	Ave. Vehicle Speed (m s⁻¹)	Ave. Vehicle Weight (Mg)	S^b (%)	M^c (%)	PM_c EF (g VKT⁻¹)	PM_{2.5} EF (g VKT⁻¹)
Observed	berm	36	N/A	N/A	N/A	N/A	64	3
	access	6	N/A	N/A	N/A	N/A	245	12
AP-42: industrial	berm	36	N/A	22	13	N/A	974	108
	access	6	N/A	2	15	N/A	388	43
AP-42: public	berm	36	4.5	N/A	13	20	137	15
	access	6	7.5	N/A	15	1	363	40

^a“N/A” (not applicable) is shown to indicate that a parameter was not used in the emission factor calculation.

^bEstimated silt content based on information in AP-42 for road type and knowledge of the berm road construction schedule.

^cEstimated moisture based on information in AP-42 for road type and based on watering of berm road.

Figure 1. Schematic of sampling scheme designed to capture fugitive fly ash particles downwind of a fly ash disposal area. Unpaved roads between the disposal site and monitoring equipment were a major source of confounding emissions.

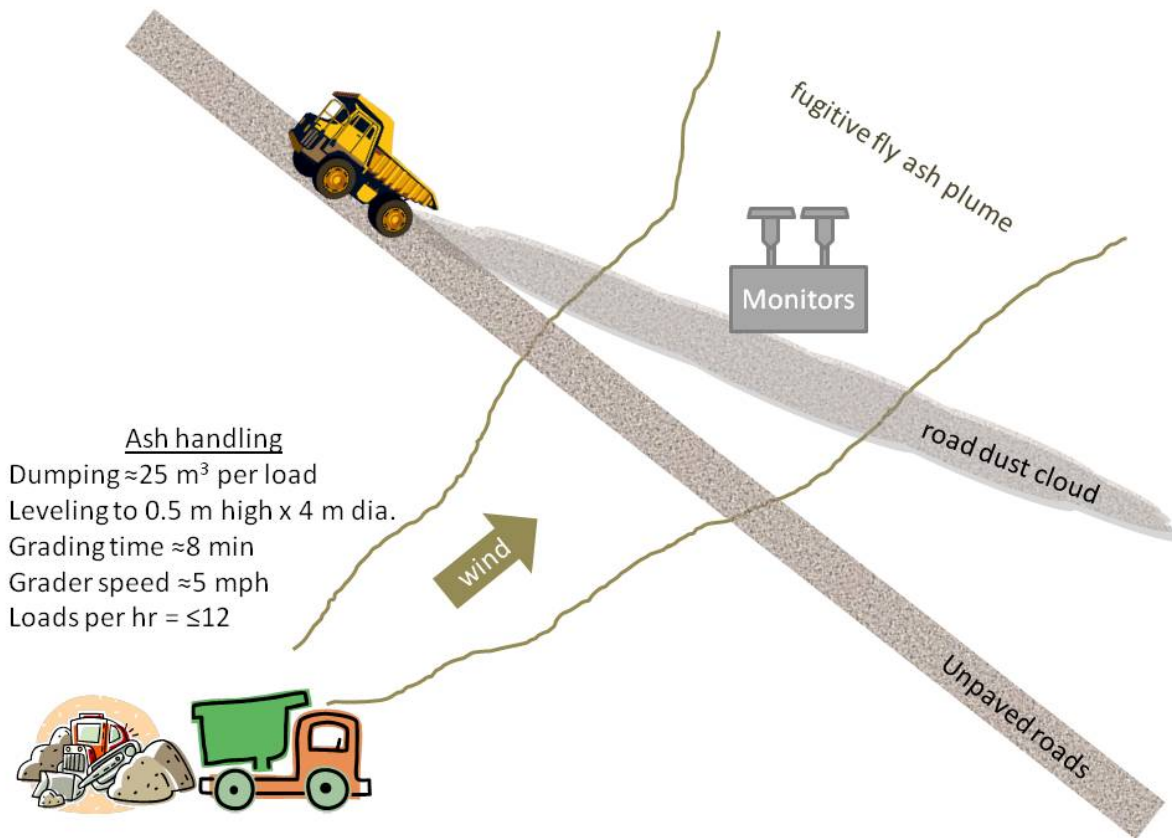


Figure 2. Aerial photograph of the area around the fly ash disposal site showing locations for various physical features and monitoring equipment. The photograph predates the study by a few years (all sides and most of the top of the fly ash dry stack were covered by vegetation during the study) and was taken when the grass was dormant. Monitoring sites 2 and 3 (triangles) are labeled. The meteorological tower is represented by a square. A cartoon camera illustrates the location of the video surveillance system. Four circles denote locations of potential ash disposal sites used in the dispersion modeling. The background monitoring site, not in this field of view, was more than 1000 m west of the dry stack.

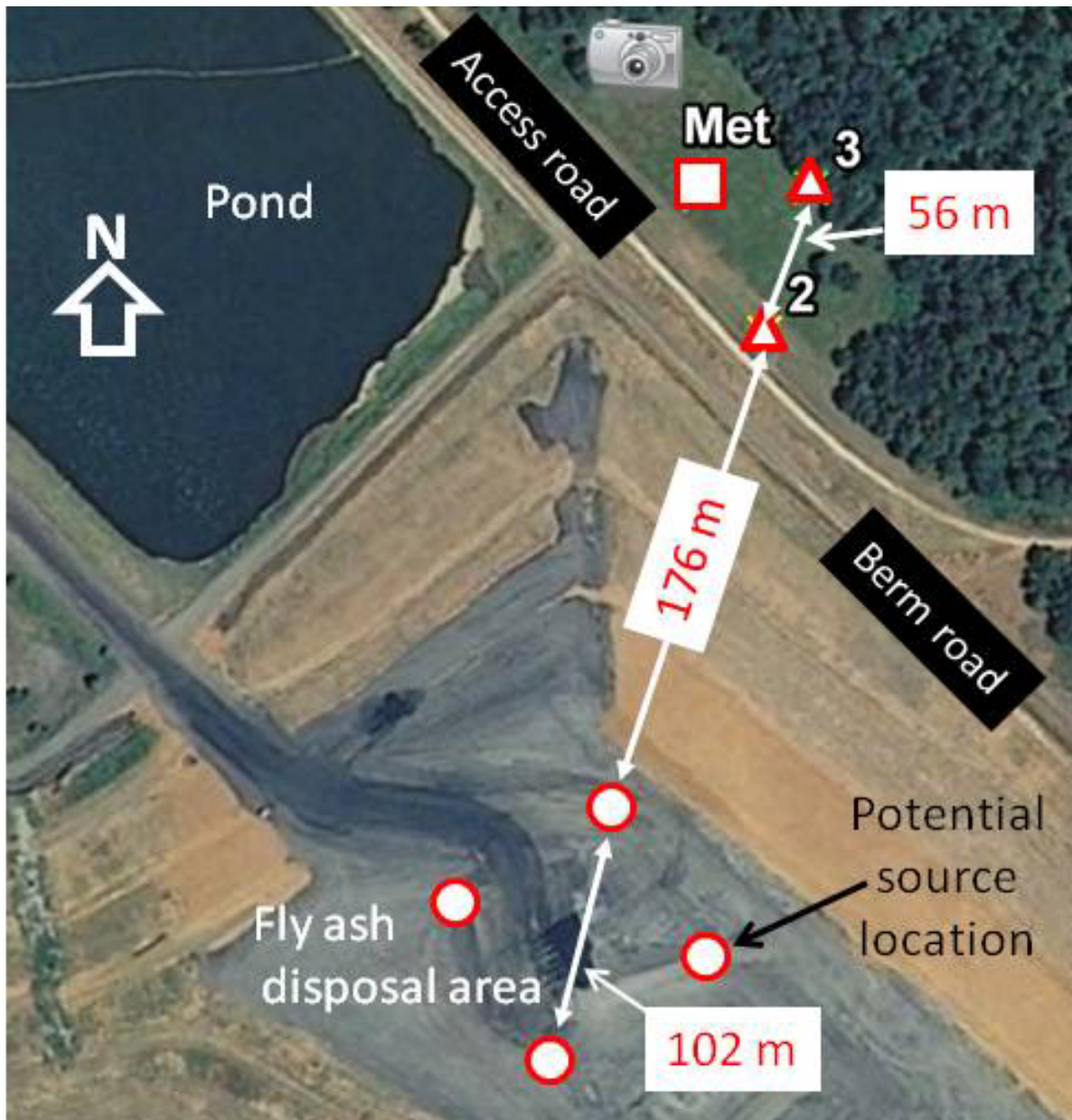


Figure 3. Frequency distributions of measured PM_{2.5} and PM₁₀ concentrations at the three monitoring sites for Monday-Friday, 07:00 through 15:00 local standard time, when fly ash was typically moved to the storage area. Mean values ($\mu\text{g m}^{-3}$) are denoted \bar{C} . All meteorological conditions are represented.

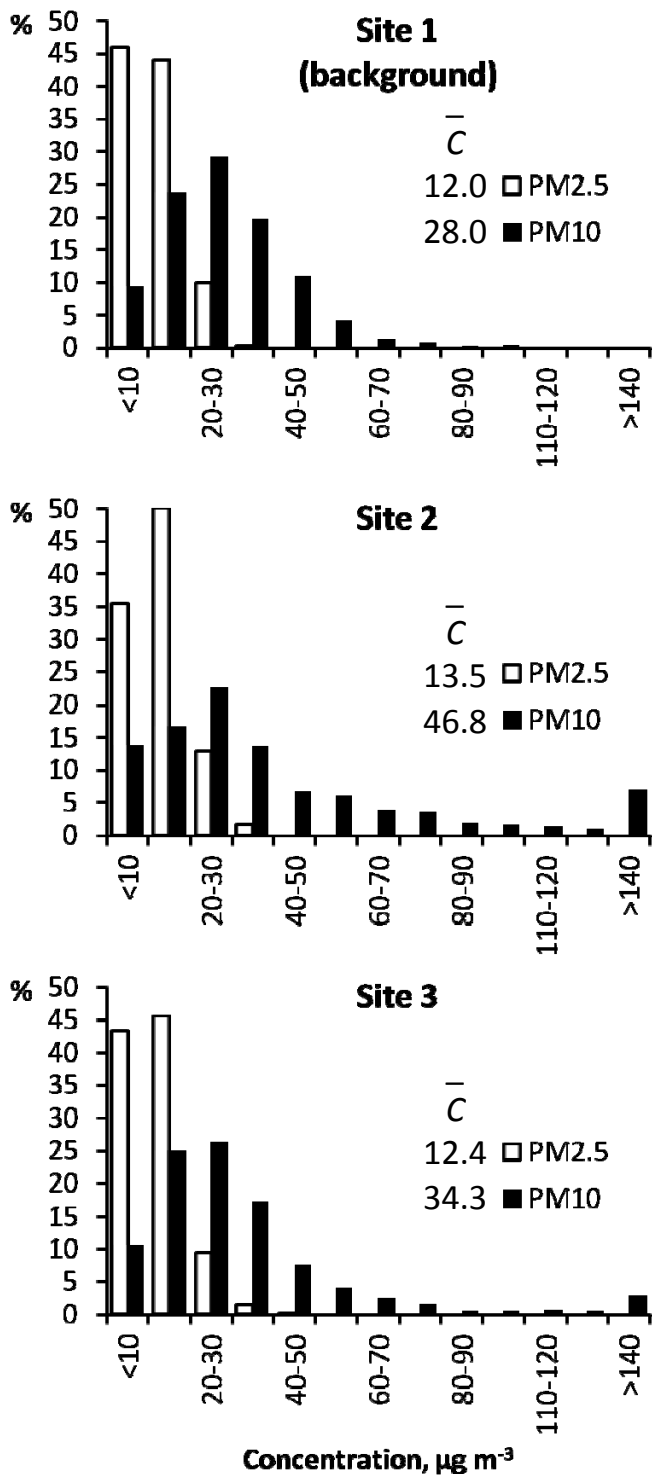


Figure 4. Distributions of “excess” fugitive fly ash plume concentrations (C_{xs}) determined for fly ash plume events captured by the particulate monitors.

